

Reconstructing the Intrinsic Triaxial Shape of the Virgo Cluster

Bomee Lee and Jounghun Lee

*Department of Physics and Astronomy, FPRD, Seoul National University, Seoul 151-747,
Korea*

bmlee@astro.snu.ac.kr, jounghun@astro.snu.ac.kr

ABSTRACT

To use galaxy clusters as a cosmological probe, it is important to account for their triaxiality. Assuming that the triaxial shapes of galaxy clusters are induced by the tidal interaction with the surrounding matter, Lee and Kang recently developed a reconstruction algorithm for the measurement of the axial ratio of a triaxial cluster. We examine the validity of this reconstruction algorithm by performing an observational test of it with the Virgo cluster as a target. We first modify the LK06 algorithm by incorporating the two dimensional projection effect. Then, we analyze the 1275 member galaxies from the Virgo Cluster Catalogue and find the projected direction of the Virgo cluster major axis by measuring the anisotropy in the spatial distribution of the member galaxies in the two dimensional projected plane. Applying the modified reconstruction algorithm to the analyzed data, we find that the axial ratio of the triaxial Virgo cluster is (1: 0.54 : 0.73). This result is consistent with the recent observational report from the Virgo Cluster Survey, proving the robustness of the reconstruction algorithm. It is also found that at the inner radii the shape tends to be more like prolate. We discuss the possible effect of the Virgo cluster triaxiality on the mass estimation.

Subject headings: cosmology:theory — large-scale structure of universe

1. INTRODUCTION

Galaxy clusters provide one of the most powerful tools to constrain the key cosmological parameters. In the era of precision cosmology, it is important to determine their mass as accurately as possible before using them as a cosmological probe. Any kind of simplified assumption about the properties of galaxy clusters could cause substantial systematics in the mass estimation. The triaxial shapes of galaxy clusters are one of such properties.

It has been long known both observationally and numerically that the galaxy clusters are noticeably triaxial (e.g., Frenk et al. 1988; West 1989; Plionis et al. 1991; Warren et al. 1992). While plenty of efforts have been already made to take into account the triaxial shapes of galaxy clusters (Jing & Suto 2002; Fox & Pen 2001; Suwa et al. 2003; Lee & Suto 2004; Kasun & Evrard 2005; Hopkins et al. 2005; Lee et al. 2005; Smith & Watts 2005; Hayashi et al. 2007), previous studies have been largely focused on the statistical treatment of cluster triaxiality. For the measurement of the gas mass fraction of galaxy clusters that can provide powerful constraints on the density parameter and the dark energy equation of state (White et al. 1993; Lubin et al. 1996; Cen 1997; Evrard 1997; Cooray 1998; Laroque et al. 2006; Ferramacho & Blanchard 2007), however, it is necessary to deal with the individual clusters and their triaxial shapes.

The standard picture based on the cosmic web theory (Bardeen et al. 1986; Bond et al. 1996) explains that galaxy clusters are rare events corresponding to the local maxima of the initial density field and form at the dense nodes of the local filaments in the cosmic web through tidal interactions with the surrounding matter. The tidal effect from the surrounding matter results in the deviation of cluster shapes from spherical symmetry as well as the preferential alignments of cluster galaxies (or halos) with the major axes of their host clusters (Binggeli 1982; Struble & Peebles 1985; Hopkins et al. 2005; Kasun & Evrard 2005; Lee et al. 2005; Algood et al. 2006; Altay et al. 2006; Paz et al. 2006).

In the frame of this standard scenario, Lee & Kang (2006, hereafter, LK06) have recently developed an analytic algorithm to reconstruct the triaxial shapes of individual clusters. The key concept of the LK06 algorithm is that the two axial ratios of a triaxial cluster are related to the eigenvalues of the local tidal shear tensor. By measuring the spatial alignment of the cluster galaxies with the major axis of their host cluster, one can determine the eigenvalues of the local tidal tensor, which will in turn yields the two axial ratios of a triaxial cluster.

Testing their analytic model against high-resolution N-body simulations, LK06 have shown that their algorithm works well within 20% errors. Now that the LK06 algorithm is known to work in principle, it is time to test the algorithm against observations. Our goal here is to apply the LK06 algorithm to real observational data and examine its validity in practice. Here, we use the Virgo cluster as a target, whose triaxial shape has been very recently measured observationally (Mei et al. 2007).

The organization of this paper is as follows. In §2, a brief overview of the LK06 algorithm is provided and how to incorporate the two dimensional projection effect into the algorithm is explained. In §3, the Virgo cluster data are analyzed and its triaxial shapes are reconstructed using the LK06 algorithm. In §4, the results are summarized, and the advantages and the

caveats of our model are discussed.

2. THEORETICAL MODEL

2.1. Overview of the LK06 Algorithm

According to the LK06 algorithm, the cluster triaxial shape originates from its tidal interaction with the surrounding matter distribution. This assumption has been verified from high-resolution N-body simulation which demonstrated clearly that the tidal field elongates the cluster shapes (e.g., Altay et al. 2006, and references therein). LK06 has shown that the two axial ratios of a triaxial cluster are related to the three eigenvalues of the local tidal tensor defined as the second derivative of the gravitational potential:

$$\frac{b}{c} = \left(\frac{1 - \lambda_2}{1 - \lambda_3} \right)^{1/2}, \quad \frac{a}{c} = \left(\frac{1 - \lambda_1}{1 - \lambda_3} \right)^{1/2}, \quad (1)$$

where $\{a, b, c\}$ (with $a \leq b \leq c$) are the three principal axis lengths of a cluster and $\{\lambda_1, \lambda_2, \lambda_3\}$ (with $\lambda_1 \geq \lambda_2 \geq \lambda_3$) are the three eigenvalues of the local tidal tensor, \mathbf{T} . According to this formula, one can estimate the cluster axial ratios if $\lambda_1, \lambda_2, \lambda_3$ is fixed by fitting the probability density distribution, $p(\cos \theta)$ analytically to the observational data. LK06 suggested that the preferential locations of the cluster galaxies near the cluster major axes given the local tidal tensor be described as

$$\langle \hat{x}_i \hat{x}_j | \hat{T} \rangle = \frac{1-s}{3} \delta_{ij} + s \hat{T}_{ik} \hat{T}_{kj}. \quad (2)$$

where $\hat{\mathbf{x}} \equiv (\hat{x}_i)$ is the unit position vector of a cluster galaxy, $\hat{\mathbf{T}} \equiv \mathbf{T}/|\mathbf{T}|$ is the unit tidal shear tensor, and $s \in [-1, 1]$ is the correlation parameter that represents the correlation strength between $\hat{\mathbf{x}}$ and $\hat{\mathbf{T}}$. Under the assumption that the minor axis of the tidal shear tensor is in the direction of the cluster major axis, equation (2) basically describes the alignment between the position of a cluster galaxy and the major axis of its host cluster. If $s = -1$, there is a maximum alignment. If $s = 1$, there is a maximum anti-alignment. The case of $s = 0$ corresponds to no alignment.

Let θ_{3d} be the angle between the host cluster major axis and the galaxy position vector. Under the assumption that the cluster major axis is in the direction of the minor principal axis of the tidal shear tensor, The probability density distribution of $\cos \theta_{3d}$ was derived by LK06 as

$$p(\cos \theta_{3d}) = \frac{|M|}{2\pi} (\hat{x}_i \cdot M_{ij}^{-1} \cdot \hat{x}_j)^{-\frac{3}{2}}, \quad (3)$$

where ϕ is an azimuthal angle of $\hat{\mathbf{x}}$ measured in an arbitrary coordinate system. Here, covariance matrix \mathbf{M} is defined as $\mathbf{M} \equiv \langle \hat{x}_i \hat{x}_j | \hat{T} \rangle$. Note that equation (3) holds good for any arbitrary coordinate system in which the tidal shear tensor is not necessarily diagonal.

In the principal axis frame of the tidal tensor, equation (4) can be expressed only in terms of the three eigenvalues of the tidal shear tensor as

$$p(\cos \theta) = \frac{1}{2\pi} \prod_{i=1}^3 (1 - s + 3s\hat{\lambda}_i^2)^{-1/2} \times \int_0^{2\pi} \left(\frac{\sin^2 \theta \cos^2 \phi}{1 - s + 3s\hat{\lambda}_1^2} + \frac{\sin^2 \theta \sin^2 \phi}{1 - s + 3s\hat{\lambda}_2^2} + \frac{\cos^2 \theta}{1 - s + 3s\hat{\lambda}_3^2} \right)^{-3/2} d\phi, \quad (4)$$

where $\{\hat{\lambda}_i\}_{i=1}^3$ are the eigenvalues of $\hat{\mathbf{T}}$, related to $\{\lambda_i\}_{i=1}^3$ as

$$\lambda_1 = \frac{\delta_c \hat{\lambda}_1}{\hat{\lambda}_1 + \hat{\lambda}_2 + \hat{\lambda}_3}, \quad \lambda_2 = \frac{\delta_c \hat{\lambda}_2}{\hat{\lambda}_1 + \hat{\lambda}_2 + \hat{\lambda}_3}, \quad \lambda_3 = \frac{\delta_c \hat{\lambda}_3}{\hat{\lambda}_1 + \hat{\lambda}_2 + \hat{\lambda}_3}, \quad (5)$$

where $\delta_c \approx 1.68$ is the linear density threshold for a dark halo (Eke et al. 1996) satisfying the following constraint of $\delta_c = \sum_{i=1}^3 \lambda_i$.

The key concept of LK06 algorithm is that by fitting equation (3) to the observed probability distribution, one can find the best-fit values of λ_1, λ_2 and s , and then determine the cluster axial ratios using equation (1). Although LK06 algorithm allows us in principle to reconstruct the three dimensional intrinsic triaxial shapes of individual clusters, it is restricted to the cases where the informations on the three dimensional positions of the cluster galaxies in the cluster principal axis frame are given. Unfortunately, for most clusters, these informations are not available but only two dimensional projected images of clusters.

In §2.2, we attempt to modify the LK06 algorithm in order to incorporate the two dimensional projection effect.

2.2. Projection Effect

Let us suppose that the position vectors of the cluster galaxies are all projected along the line of sight direction onto the plane of a sky. Unless the major axis of the host cluster is perfectly aligned with the line-of-sight direction to the cluster center, one would expect that the projected position vectors of the cluster galaxies should show a tendency to be aligned with the projected major principal axes.

Let θ_{2d} be the angle between the projected cluster major axis and galaxy position vector in the plane of sky. The probability distribution can be calculated by integrating equation

(3) along the line of sight as

$$p(\cos \theta_{2d}) = \int_{-1}^1 \frac{|M|}{2\pi} (\hat{x}_i \cdot M_{ij}^{-1} \cdot \hat{x}_j)^{-\frac{3}{2}} d\hat{x}_3, \quad (6)$$

where (\hat{x}_3) is now chosen to be in the direction of the line of sight. In other words, we consider a certain Cartesian coordinate system in which the \hat{x}_3 direction is parallel to the line of the sight to the cluster center of mass. Note that in this coordinate system the tidal tensor is not necessarily diagonal.

Through the similarity transformation

$$\hat{\mathbf{T}} = \mathbf{R}^t \cdot \hat{\mathbf{\Lambda}}_{\mathbf{T}} \cdot \mathbf{R}, \quad (7)$$

with

$$\mathbf{\Lambda}_{\mathbf{T}} = \begin{pmatrix} \hat{\lambda}_1 & 0 & 0 \\ 0 & \hat{\lambda}_2 & 0 \\ 0 & 0 & \hat{\lambda}_3 \end{pmatrix}, \quad (8)$$

one can express the nondiagonal unit tidal tensor $\hat{\mathbf{T}}$ in terms of its eigenvalues. Here, the rotation matrix \mathbf{R} has the form of (Binney 1985)

$$\mathbf{R} = \begin{pmatrix} -\sin \psi & -\cos \psi \cos \xi & \cos \psi \sin \xi \\ \cos \psi & -\sin \psi \cos \xi & \sin \psi \sin \xi \\ 0 & \sin \xi & \cos \xi \end{pmatrix}, \quad (9)$$

where (ξ, ψ) is the polar coordinate of the line-of-sight direction in the principal axis frame of the cluster.

Through equations (6)-(9), we finally find an analytic expression for the probability density distribution of $\cos \theta_{2d}$ in terms of $\{\hat{\lambda}_i\}_{i=1}^3$ and the correlation parameter s :

$$p(\cos \theta_{2d}) = \frac{(1+s)^2(1-2s)}{2\pi} \int_{-1}^1 Q^{-3/2} d\hat{x}_3, \quad (10)$$

with the factor Q defined as

$$\begin{aligned} Q \equiv & [(1+s)^2 - 3s(1+s)](A_1\hat{\lambda}_1 + A_2\hat{\lambda}_2 + A_3\hat{\lambda}_3)(1 - \hat{x}_3^2), \\ & + [(1+s)^2 - 3s(1+s)](C_1\hat{\lambda}_1 + C_2\hat{\lambda}_2 + C_3\hat{\lambda}_3)\hat{x}_3^2, \\ & + 6s(1+s)(B_1\hat{\lambda}_1 + B_2\hat{\lambda}_2 + B_3\hat{\lambda}_3)\hat{x}_3\sqrt{1 - \hat{x}_3^2}, \end{aligned} \quad (11)$$

where the coefficients $\{A_i\}_{i=1}^3, \{B_i\}_{i=1}^3, \{C_i\}_{i=1}^3$ are given as

$$A_1 = \cos \psi \cos \theta_{2d} (\cos \psi \cos \theta_{2d} - 2 \sin \psi \cos \xi \sin \theta_{2d}) + \sin^2 \theta_{2d} (\sin^2 \psi + \sin^2 \xi \cos^2 \psi),$$

$$\begin{aligned}
A_2 &= \sin \psi \cos \theta_{2d} (\sin \psi \cos \theta_{2d} + 2 \cos \psi \cos \xi \sin \theta_{2d}) + \sin^2 \theta_{2d} (\cos^2 \psi + \sin^2 \xi \sin^2 \psi), \\
A_3 &= \cos^2 \theta_{2d} + \cos^2 \xi \sin^2 \theta_{2d}, \\
B_1 &= -\sin \xi \cos \psi (\cos \xi \sin \theta_{2d} \cos \psi + \sin \psi \cos \theta_{2d}), \\
B_2 &= -\sin \xi \sin \psi (\cos \xi \sin \theta_{2d} \sin \psi - \cos \psi \cos \theta_{2d}), \\
B_3 &= \cos \xi \sin \xi \sin \theta_{2d}, \\
C_1 &= \sin^2 \psi + \cos^2 \xi \cos^2 \psi, \\
C_2 &= \cos^2 \psi + \cos^2 \xi \sin^2 \psi, \\
C_3 &= \sin^2 \xi.
\end{aligned}$$

With this new modified algorithm in the two dimensional space, we can reconstruct the intrinsic shape of a triaxial cluster halo from the observed two dimensional image.

3. APPLICATION TO THE VIRGO CLUSTER HALO

3.1. Observational Data and Analysis

The Virgo cluster is the nearest richly populated cluster of galaxies whose properties has been studied fruitfully for long (e.g., Bohringer et al. 1994; West & Blakeslee 2000, and references therein). It is known to have approximately 1275 member galaxies (Binggeli et al. 1985) and located at a distance of approximately 16.1 Mpc from us (Tonry et al. 2001) with the major axis inclined at an angle of approximately 10° with respect to the line of sight (West & Blakeslee 2000).

Near the center of the Virgo cluster is located the large ellipticity galaxy *M87* (or Virgo A). The major axis of the Virgo cluster is found to be inclined approximately 10° with respect to the line of sight direction to *M87* (West & Blakeslee 2000). We use data from the Virgo Cluster Catalogue (Binggeli et al. 1985) which compiles the equatorial coordinates of total 1275 member galaxies.

3.2. Coordinate Transformation and Projection Effect

Let r and (α, δ) represent the three dimensional distance to a member galaxy and its equatorial coordinates, respectively. Under the assumption that the position of *M87* is the center of mass of the Virgo cluster, the Cartesian coordinate of a member galaxy in the center of mass frame can be written as

$$\begin{aligned}
x_1 &= r \cos \alpha \cos \delta - x_{1va} \\
x_2 &= r \sin \alpha \cos \delta - x_{2va}
\end{aligned}$$

$$x_3 = r \sin \delta - x_{3\text{va}} \quad (12)$$

where $(x_{1\text{va}}, x_{2\text{va}}, x_{3\text{va}})$ represents the position of *M87*. The equatorial coordinates of *M87* is measured to be $\alpha_{\text{va}} = 187.71^\circ$ and $\delta_{\text{va}} = 12.39^\circ$. The distance to Virgo A, r_{va} , from us is also known to be approximately 16.1Mpc (Tonry et al. 2001; SBF survey). Thus, we have a full information on $(x_{1\text{va}}, x_{2\text{va}}, x_{3\text{va}})$.

Now let us consider a coordinate system where the third axis is in the direction of the line of sight to *M87*. Let (u, ϑ, φ) be the spherical polar coordinate of the member galaxy in this coordinate system. It can be found through coordinate transformation as

$$\begin{pmatrix} u \\ \vartheta \\ \varphi \end{pmatrix} = \begin{pmatrix} \sin \xi_{\text{va}} \cos \psi_{\text{va}} & \cos \xi_{\text{va}} \cos \psi_{\text{va}} & -\sin \psi_{\text{va}} \\ \sin \xi_{\text{va}} \sin \psi_{\text{va}} & \cos \xi_{\text{va}} \sin \psi_{\text{va}} & \cos \psi_{\text{va}} \\ \cos \xi_{\text{va}} & -\sin \xi_{\text{va}} & 0 \end{pmatrix} \begin{pmatrix} x_1 \\ x_2 \\ x_3 \end{pmatrix} \quad (13)$$

where $(\xi_{\text{va}}, \psi_{\text{va}})$ is the polar coordinate of *M87*, so that $\xi_{\text{va}} \equiv \pi/2 - \delta_{\text{va}}$.

In the plane of sky projected along the line of sight direction, the spherical polar coordinates of the member galaxy can be regarded as the Cartesian coordinates as $r \rightarrow 0$, $\vartheta \rightarrow x_l$, and $\phi \rightarrow y_l$. Basically, it represents a two dimensional projected position of a Virgo cluster member galaxy in the plane of sky with the position of *M87* as a center.

For each member galaxy from the Virgo Cluster Catalogue, we have determined the two dimensional projected position (x_l, y_l) using the given equatorial coordinates.

3.3. Virgo Cluster Reconstruction

To measure the alignments between the positions of the Virgo cluster galaxies and the projected major axis of the Virgo cluster and compare the distribution of the alignment angles with the analytic model (eq.[6]), it is necessary to find the direction of the projected major axis in the coordinate system of (x_{1l}, x_{2l}) . Equivalently, it is necessary to have an information on the polar coordinates of the line of sight, (ξ, ψ) with respect to the three dimensional principal axis of the Virgo cluster.

The seminal paper of West & Blakeslee (2000) provides us with the information on ξ i.e., the angle between the three dimensional major axis of the Virgo cluster and the line of sight direction as approximately 10° . However, we still need the azimuthal angle ψ of the major axis of the Virgo cluster.

To find the azimuthal angle ψ , we first let $\xi = 10^\circ$ and $\psi = 0$ in the analytic model (eq.[6]). It implies that we choose a certain Cartesian coordinates (x_{1p}, x_{2p}) where the angle

ψ vanishes. Then, we transform the coordinate system of (x_{1l}, x_{2l}) into this new coordinate system as

$$\begin{pmatrix} x_{1p} \\ x_{2p} \end{pmatrix} = \begin{pmatrix} \cos \psi & \sin \psi \\ -\sin \psi & \cos \psi \end{pmatrix} \begin{pmatrix} x_{1l} \\ x_{2l} \end{pmatrix}. \quad (14)$$

Here, note that $(\cos \psi, \sin \psi)$ corresponds to the projected major axis of the Virgo cluster in the (x_{1l}, x_{2l}) coordinate system. It is expected that in this new (x_{1p}, x_{2p}) -coordinate system the the observationally measured distribution should fit the analytic model (eq.[6] best.

For a given ψ , we measure the alignment angle between the projected major axis and position vector of each Virgo cluster galaxy as

$$\cos \theta_{2d} = \hat{x}_{1p} \cos \psi + \hat{x}_{2p} \sin \psi, \quad (15)$$

where $\hat{\mathbf{x}}_p \equiv \mathbf{x}_p/|\mathbf{x}_p|$. Then, by counting the number of galaxies galaxy's number density as a function of $\cos \theta_d$, we can derive the probability distribution, $p(\cos \theta_d)$. We fit this observational distribution with the analytic model, adjusting the values of λ_1, λ_2 and s through χ^2 -minimization. We repeat the whole process varying the value of ψ , and seek for the value of ψ which yields the smallest χ^2 value. As a final step, we determine the corresponding best-fit values of λ_1 and λ_2 .

Finally, we find the axial ratios of the Virgo cluster to be $a/c = 0.54$ and $b/c = 0.73$ by using equation (1) with the constraint of $\delta_c = \sum_{i=1}^3 \lambda_i$. The best-fit value of s is also determined to be -0.25 , indicating that the positions of the cluster galaxies are indeed aligned with the major axes of the Virgo cluster. Figure [1] plots the two dimensional projected positions of the Virgo cluster galaxies in the (x_{1p}, x_{2p}) -coordinate system. The arrow represents the direction of the projected major axis determined from the chosen value of ψ .

Figure 2 plots the probability distribution of the alignment angles for four different cases of ψ . In each panel, the histogram with Poisson errors is the observational distribution while the solid line represents the analytic fitting model. The dotted line stands for the case of no alignment at all. The top left panel corresponds to the finally chosen value of ψ for which the analytic fitting model and the observational result agree with each other best. The other three panels show the three exemplary cases of ψ for which the analytic fitting model and the observational result do not agree with each other well with relatively high χ^2 value.

To investigate whether the reconstructed axial ratios of the Virgo cluster changes with the radius from the center, we introduce a cut-off radius, R_{cut} , and remeasure the axial ratios using only those galaxies located within R_{cut} from the center in the (x_{1p}, x_{2p}) - coordinate system. We repeat the same process but using four different values of R_{cut} . Table 1 lists the values of the resulting best-fit axial ratios a/c and b/c , and the best-fit correlation parameter

for the four different cut-off radii of R_{cut} . As can be seen, at the inner radius smaller than the maximum one, the shape tends to be more prolate-like, consistent with recent numerical report (e.g., Hayashi et al. 2007). Note also that the value of s is consistently -0.25 , which implies the strength of the tidal interaction with surrounding matter is consistent.

Figure 3 plots the probability distributions for the four different cases of R_{cut} . The top left panel shows the case of maximum cut-off radius. As can be seen, the agreements between the analytic fitting model and the observational result are quite good even at inner radii.

4. SUMMARY AND DISCUSSION

We have modified the cluster reconstruction algorithm which was originally developed by Lee & Kang (2006) to apply it to the two dimensional projected images of galaxy clusters in practice. Assuming that unless the cluster major axes are in the line-of-sight direction, we have found that the alignments between the galaxy positions and the projected major axes can be used to reconstruct the two axial ratios of the triaxial clusters. We have applied the modified algorithm to the observational data of the Virgo cluster and shown that the reconstructed axial ratios of (1: 0.54 : 0.73) are in good agreement with the recent report from the Virgo Cluster survey (Mei et al. 2007), which proves the validity and usefulness of our method in practice.

Now that the Virgo cluster is found to be triaxial, let us discuss on the triaxiality effect on the mass estimation. For simplification, let us assume that the Virgo cluster has a uniform density. Then, the mass of the triaxial Virgo cluster with the axial ratios given as (1 : 0.54 : 0.73) is estimated to be 2.6 times larger than the spherical case since the spherical radius is close to the minor axis length of the Virgo cluster since the major axis of the Virgo cluster is very well aligned with the line of sight direction. Therefore, it can cause maximum $\sim 50\%$ errors to neglect the Virgo cluster triaxiality.

The most prominent merit of our method over the previous one is that it reconstructs directly the *intrinsic three dimensional structures* of the underlying triaxial dark matter halo using the fact that the cluster triaxiality originated from the tidal interaction. Conventionally, the triaxial shape of a cluster is found through calculating its inertia momentum tensor. This conventional method, however, is unlikely to yield the *intrinsic* shape of the underlying dark matter halo unless the target cluster is a well relaxed system. In addition, our method does not resort to any simplified assumption like the axis-symmetry or the alignment with the line-of-sight and etc.

Yet, it is worth mentioning here a couple of limitations of our method. First, it assumes

that the major axes of the clusters are not aligned with the line-of-sight direction so that the alignments between the galaxy positions and the projected major axes can be measured.

Second, for the Virgo cluster, the crucial information on the angle ξ between the three dimensional major axis and the line of sight has been already given West & Blakeslee (2000). Which simplifies the whole of our method since it was only ψ that has to be determined. For most clusters, however, this information is not given, so that both the values of ξ and ψ have to be determined through fitting before finding the axial ratios.

Third, its success is subject to the validity of the LK06 algorithm. According to the numerical test, the LK06 algorithm suffers approximately 20% errors for the case that the number of the member galaxies is not high enough. It implies that the LK06 algorithm is definitely restricted to the rich clusters with large numbers of galaxies. Therefore, it may be necessary to refine and improve the LK06 algorithm itself for the application to poor cluster samples. Our future work is in this direction.

This work is supported by the research grant No. R01-2005-000-10610-0 from the Basic Research Program of the Korea Science and Engineering Foundation.

REFERENCES

- Algood, B. et al. 2006, MNRAS, 367, 1781
- Altay, G., Colberg, J. M., & Croft, R. A. C. 2006, MNRAS, 370, 1422
- Anninos, P., & Norman, M. L. 1996, ApJ, 459, 12
- Bardeen, B., Bond, R. J., Kaiser, N., & Szalay, H. 1986, ApJ, 23, 567
- Basilakos, S., Plionis, M., & Maddox, S.J. 2000, MNRAS, 316, 779
- Binggeli, B. 1982, A&A, 107, 338
- Binggeli, B., Sandage, A., & Tammann, G., A. 1985, AJ, 90, 1681
- Binney, J. 1985, MNRAS, 212, 767
- Bohringer, H. et al. 1994, Nature, 368, 828
- Bond, J. R., Kofman, L., & Pogosyan, D. 1996, Nature, 380, 603
- Cen, R. 1997, ApJ, 485, 39
- Cooray, A. R. 1998, A&A, 339, 623
- Eke, V. R., Cole, S., & Frenk, C. S. 1996, MNRAS, 282, 263
- Evrard, A. E. 1997, MNRAS, 292, 289
- Fabricant, D., Gorenstein, P. 1983, ApJ, 267, 535
- Ferramacho, L. D., & Blanchard, A. 2007, A&A, 463, 423
- Fouque, P. S., Solanes, J. M., Sanchis, T., & Balowski, C. 2001, A&A, 375, 770
- Fox, D. C., & Pen U. L. 2002, ApJ, 574, 38
- Frenk, C. S., White, S. D. M., Davis, M., Efstathiou, G. 1988, ApJ, 327, 507
- Hayashi, E., Navarro, J. F., & Springel, V. 2007, accepted MNRAS
- Hopkins, P. F., Bahcall, N., & Bode, P. 2005, ApJ, 618, 1
- Jing, Y.P., & Suto, Y. 2002, ApJ, 574, 538
- Kasun, S. F., Evrard, A. E. 2005, ApJ, 629, 781

- Klypin, A., Cottlober, S., & Kravtsov, A. V. 1999, *ApJ*, 516, 530
- Laroque, S. J. 2006, *ApJ*, 652, 917
- Lee, J., Pen, U. L. 2001, *ApJ*, 555, 106
- Lee, J., Suto, Y. 2003, *ApJ*, 585, 151
- Lee, J., Suto, Y. 2004, *ApJ*, 601, 599
- Lee, J., Kang, Xi, & Jing, Y. P. 2005, *ApJ*, 639, L5
- Lee, J., Kang, Xi 2006, *ApJ*, 637, 561
- Lokas, E. L., Mamon, G. A. 2003, *MNRAS*, 343, 401
- Lubin, L. M., Cen, R., Bahcall, N. A., & Ostriker, J. P. 1996, *ApJ*, 460, 10
- Mamon, G. A., Sanchis, T. S., & Solanes, J. M. 2004, *A&A*, 414, 445
- Mclaughlin, D. E. 1999, *ApJ*, 512, L9
- Mei, S. et al. 2007, *ApJ*, 655, 144
- Mohr, J. J., Mathiesen, B., & Evrard, A. E. 1999, *ApJ*, 517, 627
- Nulsen, P. E. J., Bohringer, H. 1995, *MNRAS*, 274, 1093
- Paz, D. J., Lambas, D. G., Padilla, N., & Merchan, M. 2006, *MNRAS*, 366, 1503
- Plionis, M., Barrow, J. D., & Frenk, C. S. 1991, *MNRAS*, 249, 662
- Sanderson, A. J. R. 2003, *MNRAS*, 340, 989
- Schindler, S., Binggeli, B., & Bohringer, H. 1999, *A&A*, 343, 420
- Smith, R. E., & Watts, P. I. R. 2005, *MNRAS*, 360, 203
- Solanes, J. M. 2002, *ApJ*, 124, 2440
- Struble, M. F., Peebles, P. J. E. 1985, *AJ*, 90, 582
- Suto, Y., Sasaki, S., & Makino, N. 1998, *ApJ*, 509, 544
- Suwa, T., Habe, A., Yoshikawa, K., & Okamoto, T. 2003, *ApJ*, 588, 7
- Tonry, J. L. et al. 2001, *ApJ*, 546, 681

Warren, M. S., Quinn, P. J., Salmon, J. K., Zurek, W. H., ApJ, 399, 405

West, M. J. 1989, ApJ, 347, 610

West, M. J., Blakeslee, J. P. 2000, ApJ, 543, L27

White, S. D. M., Navarro, J., & Evrard, A. E., & Frenk, C. S. 1993, Nature, 366, 429

Zentner, A. R. et al. 2005, ApJ, 629, 219

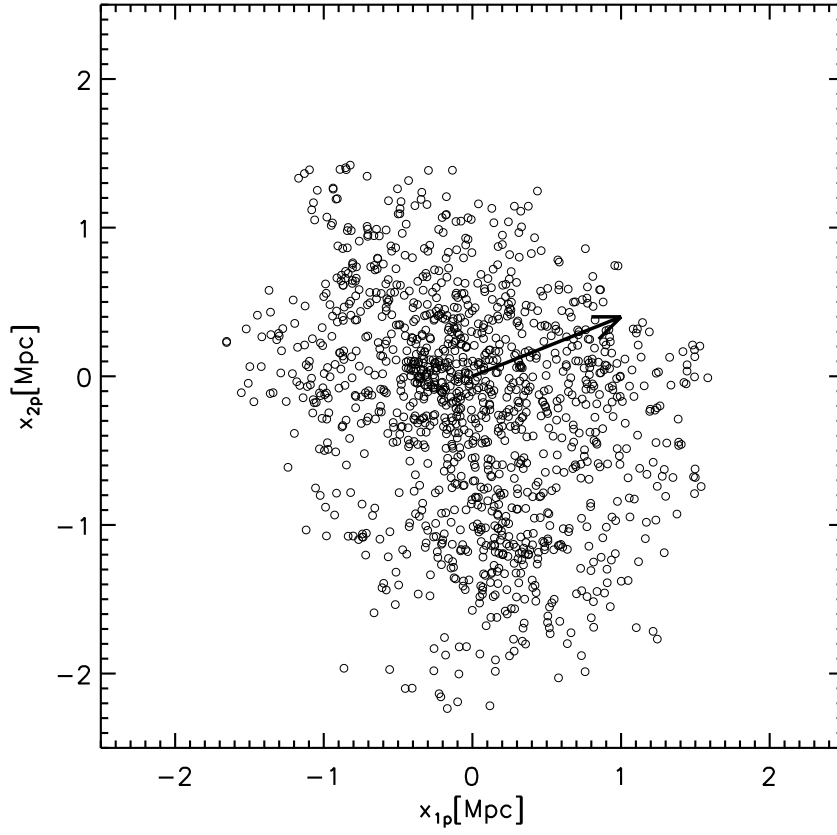


Fig. 1.— Positions of the Virgo member galaxies in the two dimensional projected space. The arrow represents the direction of the projected major axes of the Virgo cluster.

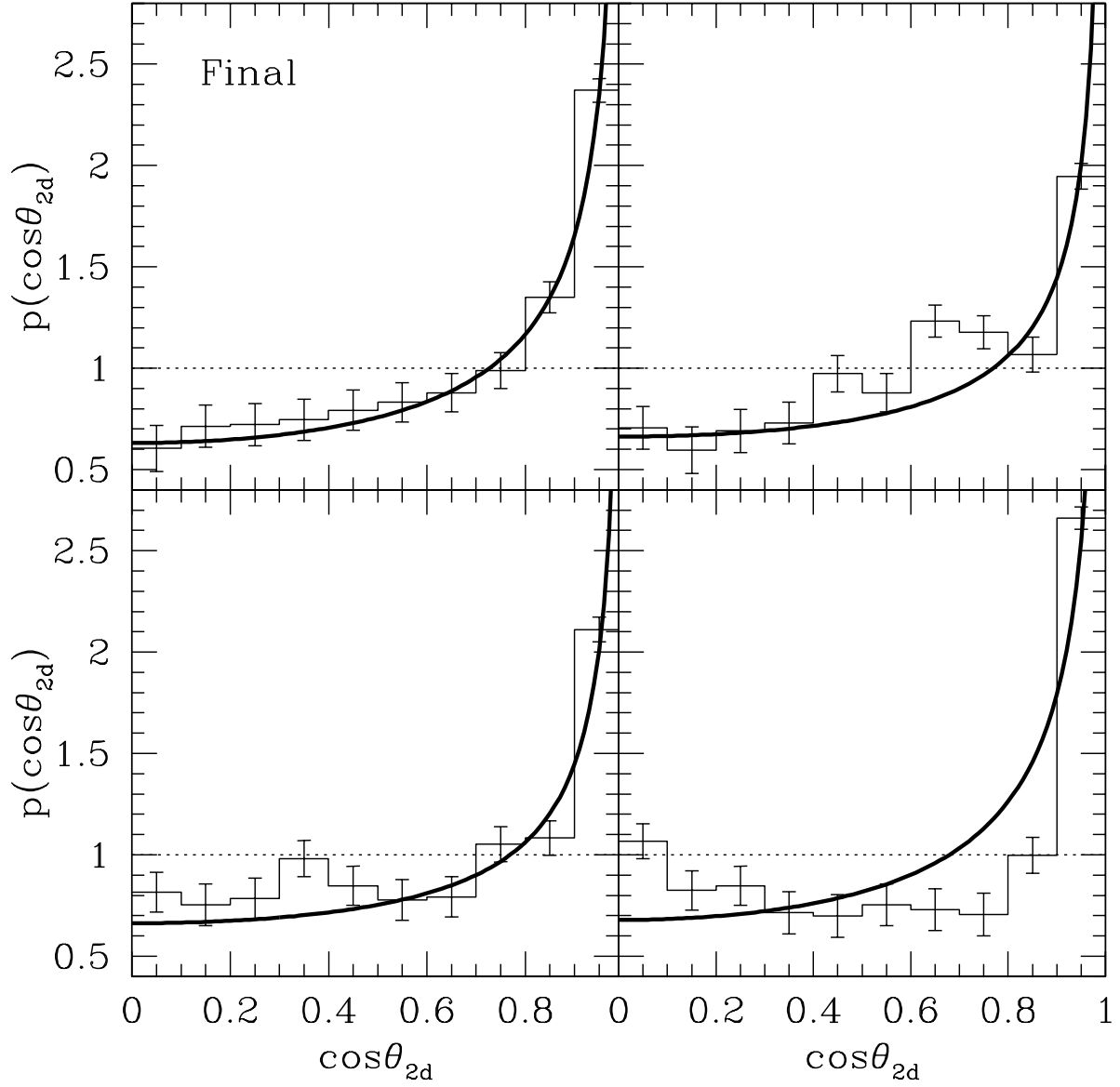


Fig. 2.— Probability density distributions of the cosines of the angles between the position vectors of the Virgo cluster galaxies and four different choices of the Virgo cluster major axis in the two dimensional projected plane of sky. In each panel, the histogram with Poisson errors represents the observational data points from the Virgo Catalog, the solid line is the analytic fitting function based on the LK06 reconstruction algorithm, and the dotted line corresponds to the case of no correlation. The top left panel corresponds to the best-fit result according to which the major axes of the Virgo cluster in the two dimensional projected plane is determined, while the other three panels show how the agreements between the observational and the analytic results change if different directions other than the major axes are used.

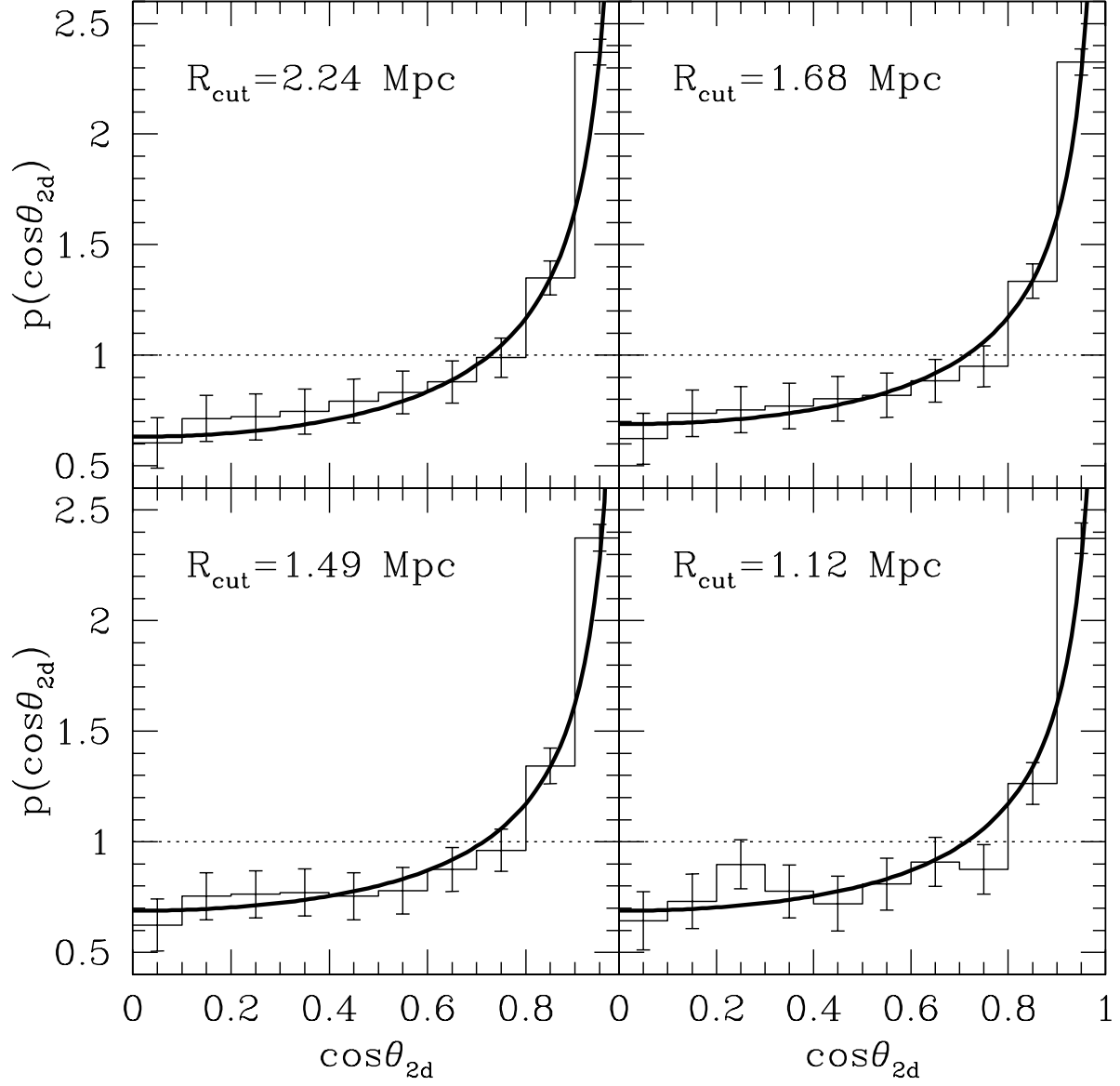


Fig. 3.— Comparison between the observational and the analytic results for the alignments at different two dimensional cut-off radii (R_{cut}).

Table 1. The cut-off radius (R_{cut}) in the two dimensional projected space, the number of the member galaxies enclosed within R_{cut} , the reconstructed two axial ratios, and the best-fit value of the correlation parameter.

R_{cut} (Mpc)	N_g	a/c	b/c	s
2.24	1275	0.53	0.73	−0.25
1.68	1221	0.64	0.69	−0.25
1.49	1154	0.64	0.69	−0.25
1.12	902	0.64	0.69	−0.25